J. Inst. Eng. India Ser. B
https://doi.org/10.1007/s40031-024-01041-y

ORIGINAL CONTRIBUTION

Performance Signature and Analysis of Patterned Surfaces Trapezoidal Patch Antenna Array with Defected Ground Structure

Suganthi Santhanam[1] · Manjunathan Alagarsamy[1] · Palavesam Thiruvalar Selvan[2] · Ahmed Nabih Zaki Rashed[3,4] · Shaik Hasane Ahammad[5] · Md. Amzad Hossain[6]

Received: 23 October 2023 / Accepted: 6 March 2024

Abstract This work proposes a microstrip antenna array with a 2 × 2 radiating trapezoidal patch with a defected ground structure (DGS) in a 30 × 70 × 1.6 mm^3 size. This design is aimed at impedance bandwidth improvement by comparing the array with a single radiating element with different DGS possibilities. The ground defected with a square-shaped structure is symmetrically etched at the center vertically on the ground between the unit elements. In the first layer of 2 × 2, the spaces between individual elements have been maintained as sufficient to minimize mutual coupling, and in the second row of the array, it has been reduced with many trials. As compared to an antenna array without DGS, the introduction of DGS shows an increase in bandwidth from 85.5 (1.84–1.93 GHz) to 123.9 MHz (2.59–2.71 GHz) without increasing its total size. DGS with a single square at the center shows the lowest return loss (− 35 dB) at the highest operating frequency (2.87 GHz), with an operating band of 2.81–2.93 GHz.

Keywords Defected ground structure · Gain · Impedance bandwidth · Surface current · Far-field pattern · Biomedical applications

Introduction

Antennas for multiple input/multiple output (MIMO) [1] with microstrip arrays are nowadays best suited for high-performance wireless communication. Modern internet apps tune to specific frequencies by means of Wireless Fidelity (Wi-Fi) relays, which support many wireless applications. Microstrip antennas, which provide proper matching with suitable frequencies, are widely used for internet applications due to their low cost and compact profile [2]. Microstrip antennas contain a radiating patch in a rectangular, circular, or other unique shape. The substrate has now been the focus of much research to cover one or more frequencies [3]. High gain [4], easy fabrication [3], and wider bandwidth [5]

✉ Ahmed Nabih Zaki Rashed
ahmed_733@yahoo.com

✉ Md. Amzad Hossain
mahossain.eee@gmail.com

Suganthi Santhanam
tvssugi@gmail.com

Manjunathan Alagarsamy
manjunathankrct@gmail.com

Palavesam Thiruvalar Selvan
thriuvalar@gmail.com

Shaik Hasane Ahammad
ahammadklu@gmail.com

[1] Department of Electronics and Communication Engineering, K. Ramakrishnan College of Technology, Trichy, Tamil Nadu 621112, India

[2] Department of Electronics and Communication Engineering, SRM TRP Engineering College, Trichy, Tamil Nadu, India

[3] Electronics and Electrical Communications Engineering Department, Faculty of Electronic Engineering, Menoufia University, Menouf 32951, Egypt

[4] Department of VLSI Microelectronics, Saveetha School of Engineering, Saveetha Institute of Medical and Technical Sciences (SIMATS), Saveetha University, Chennai, Tamilnadu, India

[5] Department of ECE, Koneru Lakshmaiah Education Foundation, Vaddeswaram 522302, India

[6] Department of Electrical and Electronic Engineering, Jashore University of Science and Technology, Jashore 7408, Bangladesh

Published online: 30 March 2024

make the Vivaldi antenna more suitable than other-shaped microstrip antennas for wireless millimeter-wave communication. The transmission capacity of Vivaldi antennas can be further improved by the proper selection of radiating shape combinations like comb-shaped slits and radiating section nesting [6].

By introducing alternative forms to flaws in the ground, microstrip array antennas intended for 5G (Fifth Generation) communications systems can perform better [7–10, 10], and [11]. Previous research has suggested a number of techniques to increase the isolation between elements in an array without making the microstrip antennas larger overall [1]. The large space requirement due to periodic structure and expensive fabrication in EBG bring much attention to defected ground structure (DGS) [12]. By creating holes and slots in the ground with different shapes, such as spirals, one can lessen the reciprocal interaction between the elements [13], C [14], V [15], U [16], and H shapes [17], ring [18], and dumbbell [19] at selected positions in the ground.

DGS, started in 1999 [20], introduces disturbances in radiating current or in the ground planes to improve antenna performance [21]. Not only for bandwidth enhancement, DGS can also be used for UWB (Ultra-WideBand) notch band introduction [22], to isolate high polarization [23], for dual-frequency applications [24], mutual coupling reduction [25], and multi-band applications [26]. Though the backward radiation leads to constraints on applications, DGS can be widely used in amplifiers [27], antennas [28], and filters [29] for enhancing the selected behavior of devices.

The recent research has been analyzed as follows: One way to decrease the mutual coupling between elements is to introduce ground defects with different shaped holes and slots. For example, one can place a dumbbell slot at a specific position in the ground and use two parallel coupled line resonators (PCR) to decouple in a two-element array with a U shape [16]. The optimization procedure for the shape and location of DGS in an inverted F-planar antenna has been presented in [30]. Though various feeding techniques like aperture coupling, proximity coupling, and coaxial probes are frequently used due to their ease of integration and fabrication [31], in order to reduce size, microstrip antenna arrays were introduced in [32] for use in the S band at 2.2 GHz on Duroid substrate, but the size miniaturization increases the cost of gain reduction. Two patches with slot-array DGS parallel to each antenna element on the ground plane have been presented in [33] for mutual coupling reduction, but with a bigger size of 120×205 mm^2. The DGS has been used to improve the gain [34] and reduce the magnitude and number of side lobes as well.

It was suggested in [35] to use a triple-layered patch antenna that has two slots carved into the bottom layer of the structure to provide a steady, symmetrical radiation pattern with a large bandwidth. In order to lessen the mutual coupling across dual-feed sites of circularly polarized microstrip antennas with an optimal axial ratio, a T-shaped defective ground structure (DGS) is given in [36]. In order to improve communication capacity in various applications, multi-input and multi-output (MIMO) antennas [37–39] were created in [40]. However, they also introduce coupling issues between array members, which would negatively impact their performance. In [41], a double-layered DGS arrangement is suggested as a compact antenna design solution for microstrip patch antennas. The equivalent circuit model is used to analytically explain the size reduction that results with the additional resonating LC elements. A metamaterial-inspired antenna array with DGS and subwavelength slots is suggested in [42] for use in the millimeter-wave to terahertz (THz) spectrums. A microstrip wire connects each radiating element in the array to the others.

To add to the literature on bandwidth enhancement methods, in this paper, we have proposed a simple, low-cost, low-profile trapezoidal-shaped microstrip antenna array with different DGS. With a square-shaped defect, the array that is being exhibited is created on an inexpensive FR4 substrate, which employs a significant improvement in bandwidth. By comparing two DGS array antennas with a single radiation patch of the same shape and same dimension, the operating frequency shift (from 1.77 to 2.87 GHz), reduction in return loss (from -26 to -36 dB), improvement in bandwidth (from 85 to 121 MHz), increase in E-field (from 15,654 (V/m) to 35,492 (V/m)), and increase in H-field (from 56 (A/m) to 149 (A/m)) have been achieved in the trapezoidal patch antenna array (TPAA) with single-square etching in the ground.

Antenna Structure and Dimensions

According to the analytical study, obtaining resonance is mostly independent of the patch width, and by utilizing mathematical modeling and previously developed mathematical formulas, one may determine the patch width for a given frequency. Apart from the width W, the radiating patch's length W has a dominant impact on the antenna's performance.

$$W = \frac{c}{2f_0}\sqrt{\frac{\varepsilon_r + 1}{2}} \tag{1}$$

$$L = \frac{c}{2f_0\sqrt{\varepsilon_r}} - 2\Delta L \tag{2}$$

The width and length of the radiating patch in (1) and (2), respectively, are denoted by W and L, wherein c is the speed of light, f_0 is the center frequency, ε_r is the relative

dielectric constant, and ΔL is the change in length. It is possible to formulate the effective dielectric constant, ε_{eff}, as

$$\varepsilon_{\text{eff}} = \frac{1}{2}(\varepsilon_r + 1) + \frac{1}{2}(\varepsilon_r - 1)\sqrt{\left|\left(1 + \frac{10h}{W}\right)\right|} \tag{3}$$

where h represents the substrate thickness. The antenna's electrical dimension appears bigger than its physical dimension due to the fringing field surrounding the radiating patch. The following illustrates how the fringing field's action changes the length of ΔL:

$$\Delta L = 0.412h \frac{(\varepsilon_e + 0.3)\left[(W/h) + 0.264\right]}{(\varepsilon_e - 0.258)\left[(W/h) + 0.8\right]} \tag{4}$$

The extant formulas are suitable for traditional rectangular radiating patches; nevertheless, the suggested antenna's geometric dimensions and form were attained through the process of modification, testing, and operation. Enhanced impedance matching throughout the operational frequency bands is achieved by optimizing the microstrip line's dimensions through design and simulation.

With optimized measurements as indicated in Table 1, the suggested trapezoidal patch antenna array (TPAA) is seen in Fig. 1. Using a FR4 substrate with 4.3 permittivity, 1.6 mm thickness, 0.025 loss tangent, and a 0.025-mm-thick copper conductor, the suggested construction is sketched out. As seen in Fig. 1a, the optimal dimension of the array front view has been determined to be whole ground at first and half ground up to the radiation edge. To achieve compact size, the front view is tried with a 2×2 array of the same size, four trapezoidal-shaped radiating elements with full ground, as shown in Fig. 1b.

With FR4 substrate on one side and 0.025-mm copper foil on the other, the finished 2×2 TPAA has dimensions of $30 \times 70 \times 1.6$ mm^3. Finally, the same front view is retained as in Fig. 1b, and DGS is introduced at the center with single-square etching as in Fig. 1c and with two additional squares as shown in Fig. 1d. The four structures considered for comparison are summarized below:

Table 1 Dimensions (in mm) of the proposed structure

Parameter	Value	Parameter	Value	Parameter	Value
W	30	L	70	W4	15
Wf	7	Lf	20	L5	2
G	05	L_{tri}	44	L4	10
Wp	10	Lp	21	W2	6.5
W1	2.5	L1	6	L2	7

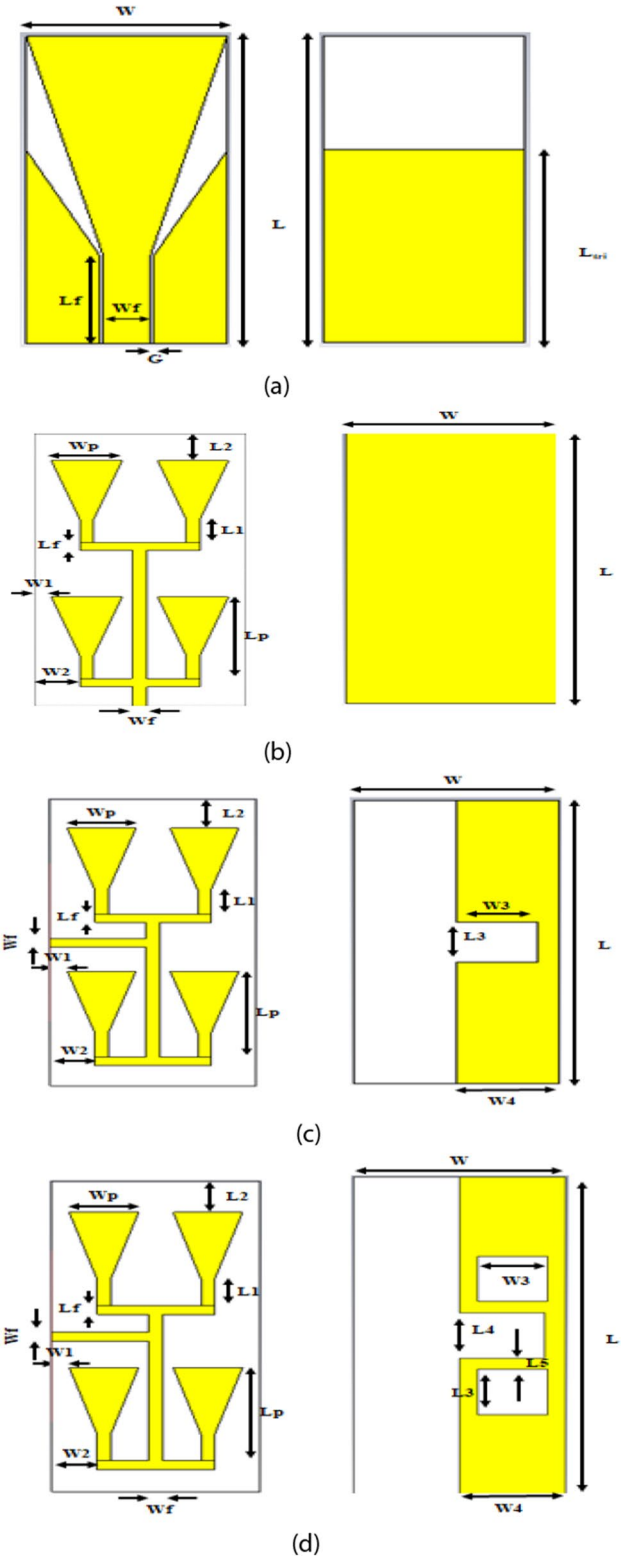

Fig. 1 Proposed TRAA with front and back views having **a** single element half ground up to radiation edge, **b** full ground, **c** partial ground DGS, **d** partial DGS with additional squares

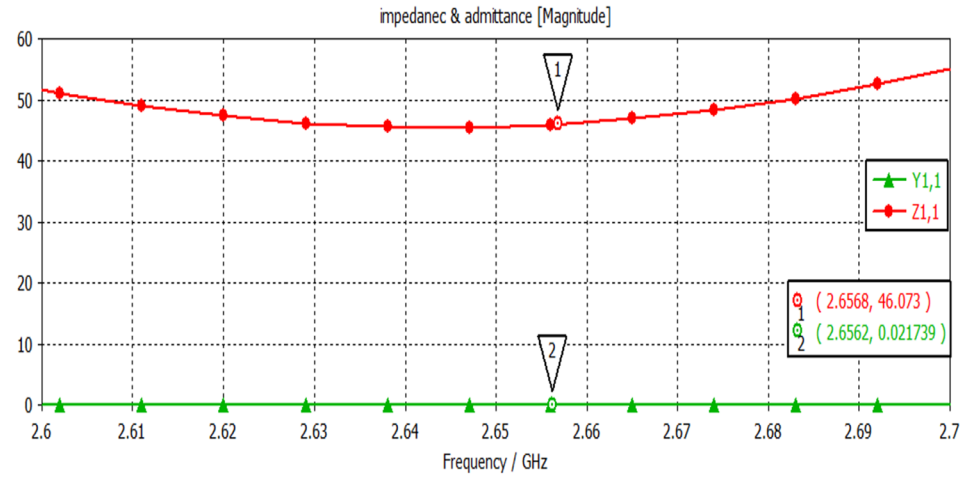

(a)

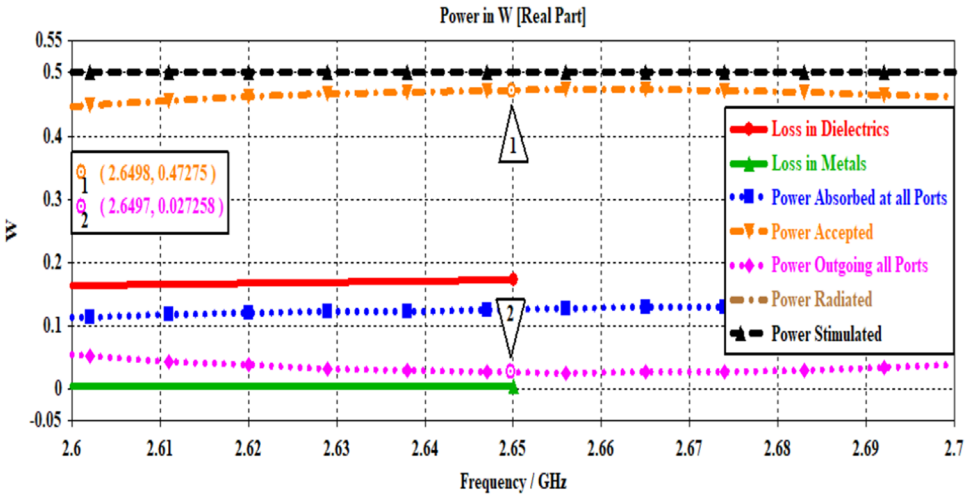

(b)

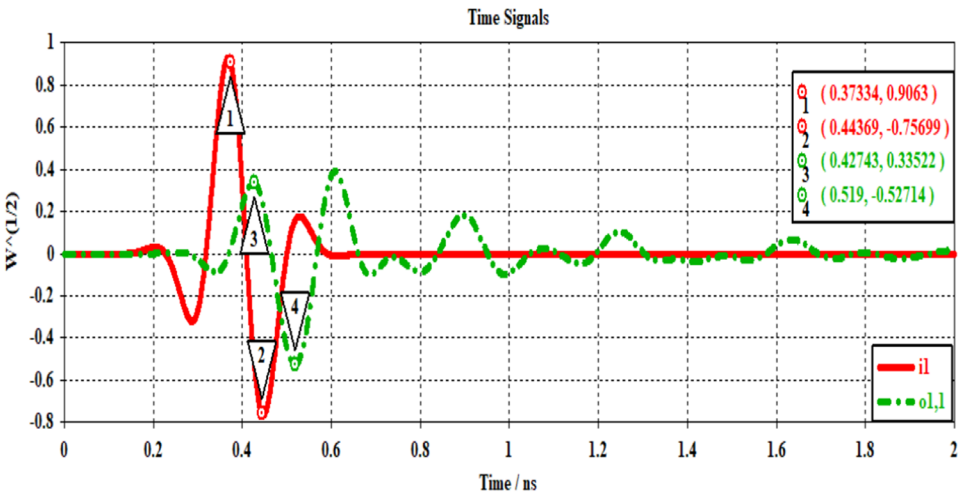

(c)

Fig. 2 **a** Z and Y comparison, **b** power and loss simulation, **c** time signals of array with half ground and DGS having additional squares

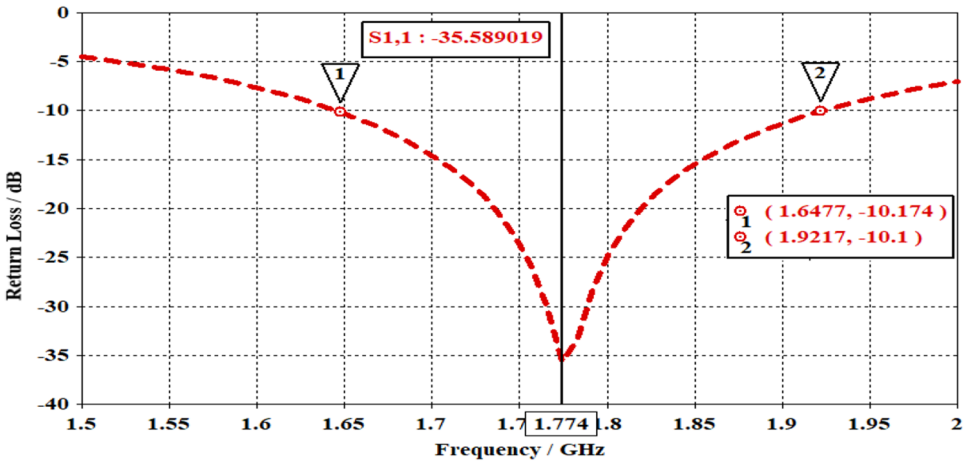

(a)

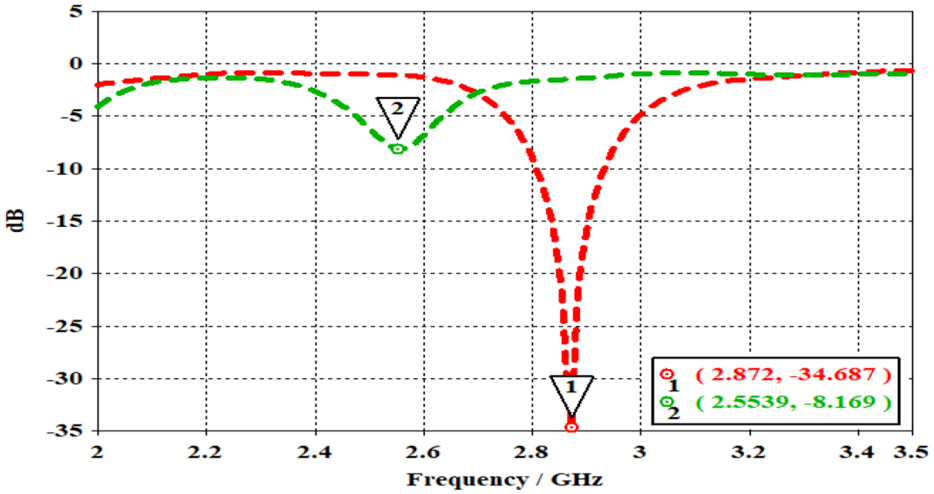

(b)

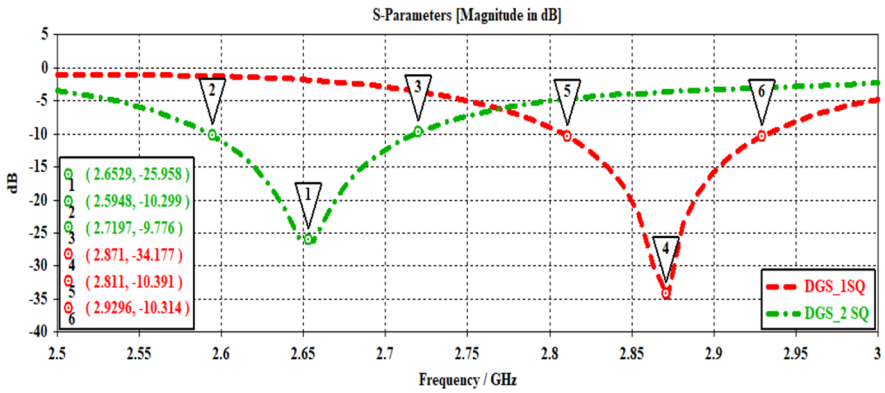

(c)

Fig. 3 Simulated return loss and VSWR of TRAA with **a–d** half ground, **b** and **e** full ground and DGS, **c** and **f** comparison for two DGS, respectively

- Figure 1a: Basic antenna with single trapezoidal patch and ground up to radiating edge of dimension $30 \times 70 \times 1.6$ mm^3.
- Figure 1b: 2×2 TPAA of the same dimension as in Ant.1 with bottom fed and full ground.
- Figure 1c: TPAA with similar front panel as in Ant.2, center fed and single-square DGS at center.

Fig. 3 (continued)

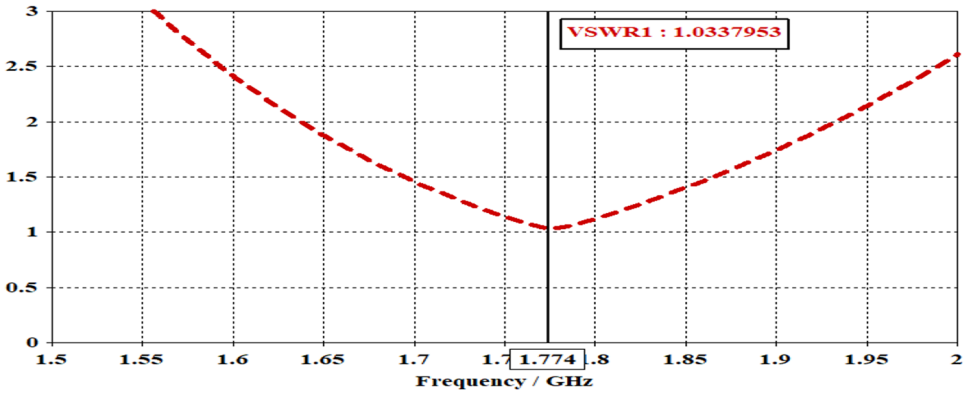

(d)

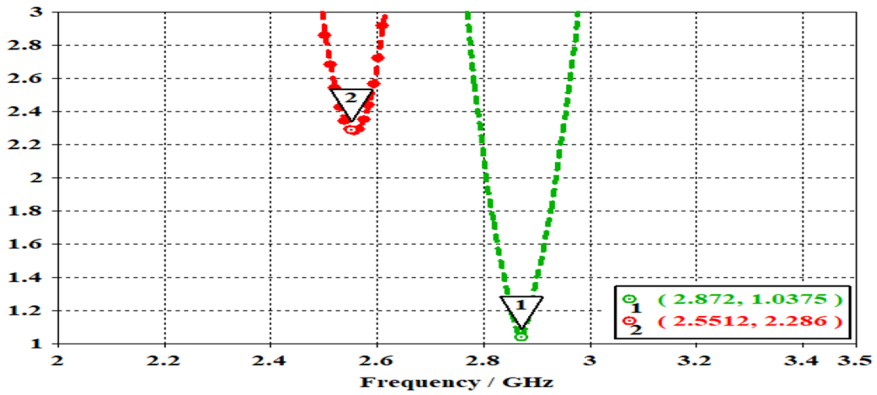

(e)

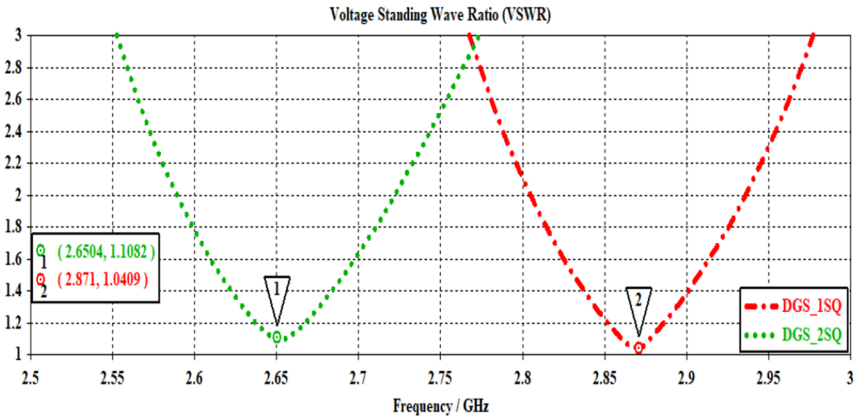

(f)

- Figure 1d: TPAA with similar front panel as in Ant.3, center fed and two additional squares on both sides of single-square DGS as in Ant.3.

Results and Discussion

The four configurations of antennas designed have been simulated using CST software to analyze their electrical properties. The antenna consists of approximately 50-Ω impedance microstrips fed at the input port.

To retain a good trade-off between the loss and power propagation of two impedances of 30 Ω and 77.5 Ω, the middle characteristic impedance of 50 Ω has been analyzed in terms of impedance, admittance, power, loss, and time signals for the antenna array, with DGS having additional squares as shown in Fig. 2. From Fig. 2a, it is clear that for a single element half ground up to the radiation edge

at 2.65 GHz, the input impedance is maintained nearly at 46.03 Ω. At this resonant frequency, the power received is equal to 0.5 W, with minimum power absorption at the input port (0.472 W) and other ports (0.027 W), as depicted in Fig. 2b. Good impedance matching between input and output has been evident, with negligible phase delay (0.15 W) at output and minimum reflection at the feeding point, as shown in Fig. 2c.

The simulated return loss and VSWR are compared, as seen in Fig. 3, to guarantee the least reflection of the proposed antenna array. It is evident from Fig. 3a that a single-element TRAA with half ground up to radiation edge operates at 1.77 GHz with a − 36-dB return loss, 274 MHz of bandwidth, and a 1.034 VSWR.

The resonance frequency is 2.55 GHz, with an unsatisfactory retune loss when the ground is fully at the array's backside. At the working frequency of 2.872 GHz, it has improved to − 34.87 dB when DGS with partial ground has been introduced, as shown in Fig. 3b**.** Further analysis has been made with the introduction of additional squares in the ground, and operating bandwidth improvement up to 123 MHz has been achieved with return loss (− 35 dB), and VSWR (1.03) at 2.87 GHz has been achieved and is improved up to 418 MHz for array with DGS having additional two squares as depicted in Fig. 3c.

The validation of these analyses has been done in terms of VSWR with an acceptable value below 1.1 for all structures, as shown in Fig. 3d–f for all structures. The size of the ground plane did not significantly determine the performance of the antenna from the standpoint of impedance matching and VSWR; rather, the antenna's location on the ground plane did matter more. The array with a complete ground plane has a lower value for its VSWR (1.033 at 1.77 GHz), and the array with a DGS having a single square in the ground has a value of 1.04 at 2.87 GHz, which is better with respect to the higher resonant. The VSWR has not varied much among the proposed structures.

The surface current distribution for each of the four structures in Fig. 4 has been simulated in order to examine the isolation behavior of the proposed DGS. The current density is lower (44.26 A/m) in an array with half ground for a single element and 133.10 A/m in an array with complete

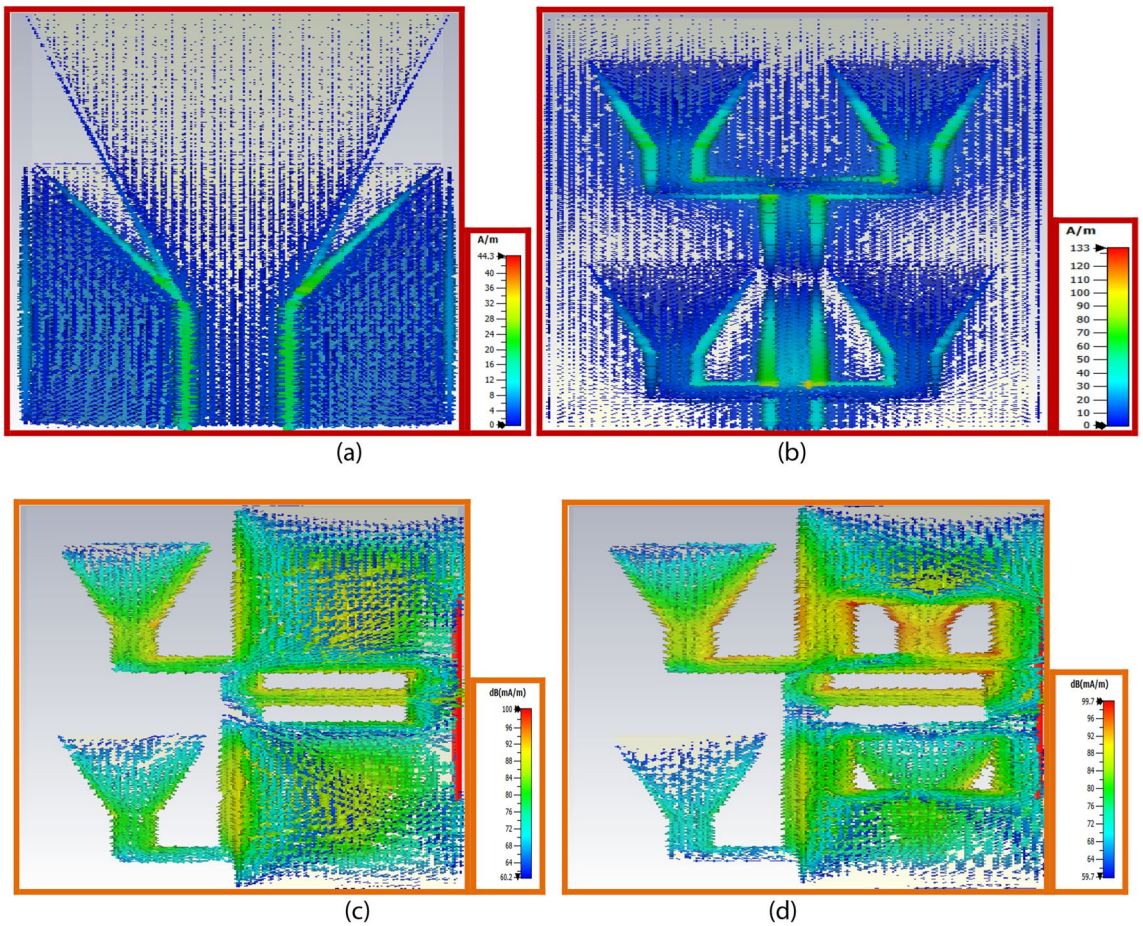

Fig. 4 Simulated current distribution of proposed structures **a** single trapezoidal element, **b** array of four elements, **c** array with DGS, **d** array with DGS and additional square at ground

ground, according to these perspectives in Fig. 4a and b. The array with DGS has achieved a 100.22 A/m current density for a single square, compared to a 99.68 A/m value with more etching using two squares in the ground, as depicted in Fig. 4c and d**,** respectively. Hence, it is clear that there is no deviation in current density with more etching in the ground.

Figure 5 shows the radiation pattern of four structures at their respective resonant frequencies for the E-plane and

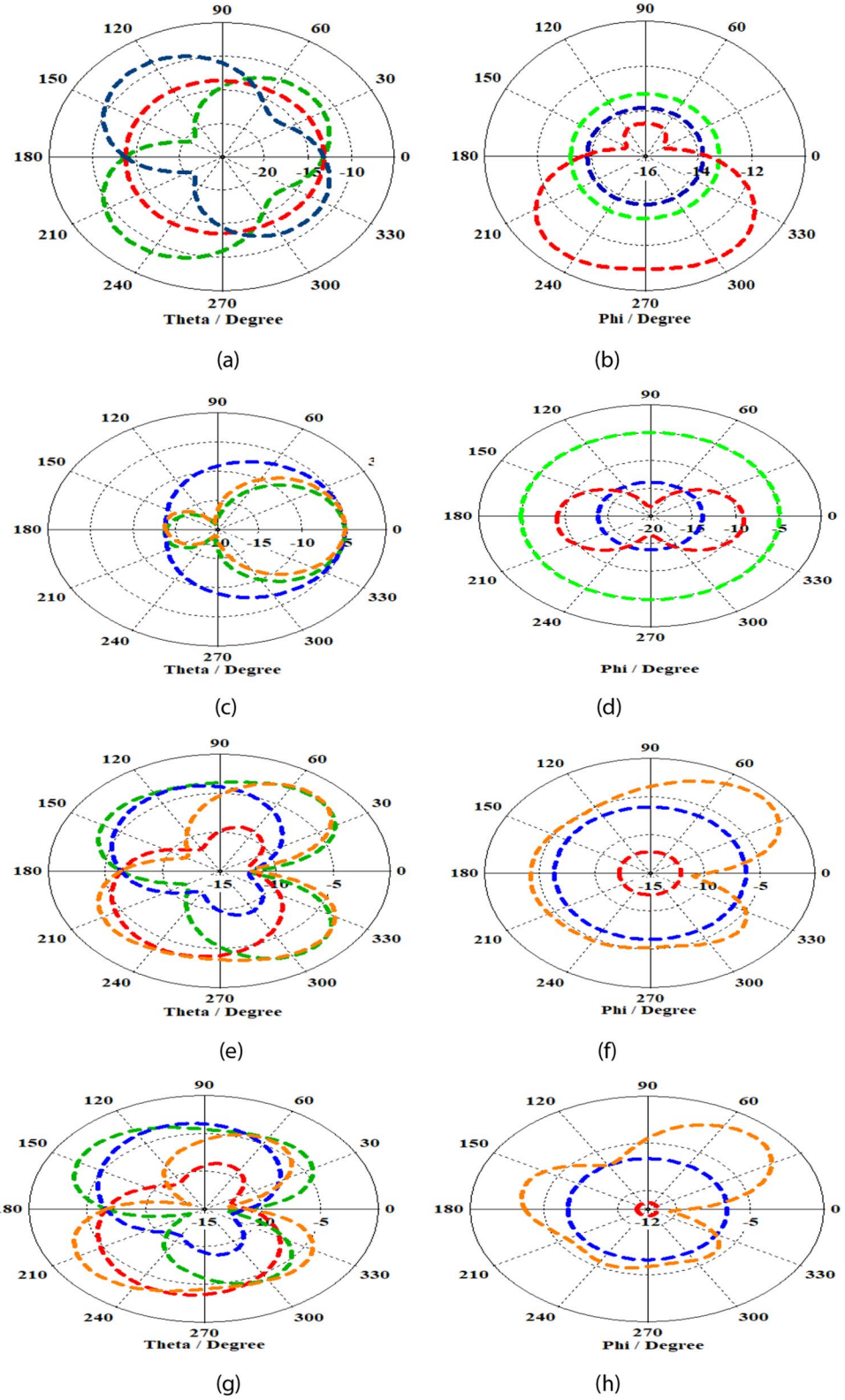

Fig. 5 H-plane and E-plane far-field polar patterns of the suggested structures **a** single element partial ground, **b** array with full ground, **c** array with DGS, **d** array with DGS and additional squares

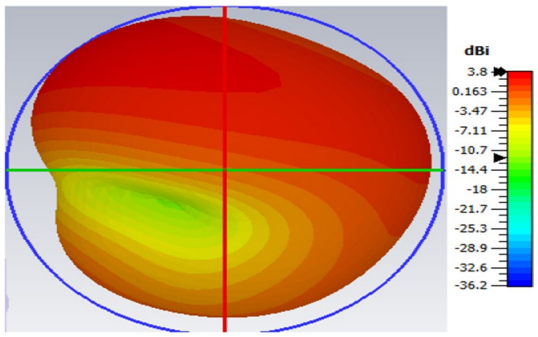

Fig. 6. 3D radiation pattern of two-square DGS antenna array

Table 2 Performance comparison of four structures proposed in this work

Parameters	Ant.1	Ant.2	Ant.3	Ant.4
Return loss (dB)	−35.58	−26.18	−34.69	−26.15
Operating/cutoff frequency (GHz)	1.774	1.891	2.872	2.656
Operating bandwidth (MHz)	274	85.5	121.6	123.9
VSWR	1.034	1.103	1.0375	1.1036
Surface current (A/m)	44.26	133.10	100.22	99.68
Directivity (dBi)	4.175	4.980	3.920	3.80
Side lobe level (dB)	−3.8	−8.8	−0.9	−1.9
Main lobe direction (deg)	−55	4	−51	141
H-field (A/m)	56.63	160.52	149.83	129.58
E-field (V/m)	15,654	36,093.4	35,492.9	44,156.5
Impedance BW %	15.44	4.521	4.233	4.66

H-plane. Figure 5a and b shows the gain plot for a half-ground single radiating electromagnetic antenna for T and θ of 0°, 90°, 180°, and 270°. The data indicate that the side lobe level is −3.8 dB with a 55° main lobe orientation. Likewise, Fig. 5b–d shows the gain for an array with two squares, a full-ground four-element array, and an array with a sine square. It is evident from the comparison that antenna arrays featuring a single-square DGS produce superior outcomes in terms of minimal side lobe level (−0.9 dB), higher directivity (3.92 dB), and maximum E-field strength. Though the gain has not increased much, we are able to retain the maximum gain of 4.98-dBi DGS for bandwidth improvement. The gain has not been compromised for the improvement of bandwidth and has been maintained from 3.92 to 3.8 dBi for DGS with single- and two-square DGS.

The two-square DGS antenna array's 3D far-field radiation pattern at 2.65 GHz, with a maximum gain of 3.8 dBi, is displayed in Fig. 6. It shows that the maximum gain has been spread out in most of the region, which is indicated by the red color, with the gain above −18 dBi in the lower region below the center. The outer region covers the maximum gain, and gain converges to the minimum value toward the center. The electrical parameters of four structures simulated in this paper are compared in Table 2.

Table 2's comparison makes it evident that we have achieved compactness by combining four radiating elements in the same $30 \times 70 \times 1.6$ mm^3 dimension with bandwidth improvement and gain maintenance. Hence, we conclude that we achieved a compact size, high bandwidth, and good radiation antenna array for low-frequency airport surveillance radar applications from 2.65 to 2.93 GHz, specifically for modem uplink transmission at 2.8 GHz. Table 3 presents a written comparison of the different radio antennas and our suggested constructions' performance. From this table, it is delineated that our proposed trapezoidal transmitting shape achieves the highest elevated 3-dB transfer speed with a single component (85.5 MHz) and encourages the transfer speed

Table 3 Comparing this work's performance to that of other arrays in references (NS: Not Specified)

Ref.	Size	DGS shape	10-dB BW (MHz)	Return Loss (dB)	F (GHz)	Substrate	Gain (dB)
[31]	1×3	T-shaped	86	−25	4	FR4	3.94
[30]	1×3	Circular meandered rings	116	−19	2.5	FR4	3
[34]	1×2	Slot	617	−48	5.8	Dielectric	6.7
[32]	2×1	Reduced ground	100	−17	2.4	RT Duroid	1.93
[33]	1×2	Slot	NS	−31	1.25	Taconic	0.3
[16]	1×2	U shape	350	−30	2.45	FR4	NS
This work	2×2 (Ant.2) (Ant.2)	Square	85.5	−26	1.89	FR4	4.98
	2×2 (Ant.3)		121.6	−34	2.87	FR4	3.92
	2×2 (Ant.4)		123.9	−26	2.66	FR4	3.8

to be expanded to 123.9 MHz for clusters in the same measurement.

Conclusions

The proposed work shows that the antenna array with a single-square DGS achieves a higher operating frequency of 2.87 GHz, a minimum return loss of − 35 dB, and a 0.12-GHz bandwidth with low cost and size, a simple profile, and easy configuration for compact wireless devices. The maximum impedance bandwidth of 274 MHz is achieved by adding ground up to the radiating edge structure, with a minimum bandwidth of 86 MHz in the full-ground array. Since the structure is compact and the FR4 substrate is low-cost, low-frequency applications between 1.77 and 2.65 GHz can make use of the suggested antenna arrangement. In future, our antenna array will be designed for flexible materials for biomedical applications and tested for verification.

Authors Contribution SS, MA, and PTS participated in conceptualization, supervision, and validation; ANZR, SHA, and MAH were involved in data curation, formal analysis, and investigation; SS, MA, PTS, and ANZR helped with methodology, visualization, and writing—original draft; MAH and ANZR helped with resources and software; and SS, MAH, MA, SHA, and ANZR were involved in writing—review and editing.

Funding Not applicable.

Availability of data and material Not applicable.

Declarations

Conflict of interest No competing interests.

Ethics approval Not applicable.

Consent to participate Not applicable.

Consent for publication Not applicable.

References

1. Y.K. Gupta, A. Goel, A. Tiwari, A.S. Das, *Performance analysis of high-speed MIMO FSO system in various data formats*, in *2023 1st International Conference on Innovations in High Speed Communication and Signal Processing (IHCSP), BHOPAL, India* (2023), pp. 398–401. https://doi.org/10.1109/IHCSP56702.2023.10127215
2. D. Rusdiyanto, C. Apriono, D. Widi, A. Muslim, Bandwidth and gain enhancement of microstrip antenna using defected ground structure and horizontal patch gap. Sinergi **25**(2), 153–158 (2021)
3. D. Huang, Z. Du, Y. Wang, A quad-antenna system for 4G/5G/GPS metal frame mobile phones. IEEE Antennas Wirel. Propag. Lett. **18**(8), 1586–1590 (2019)
4. S.S. Zhu, H. Liu, H. Liu, Z. Chen, H. Xu, Vivaldi antenna array using defected ground structure for edge effect restraint and back radiation suppression. IEEE Antennas Wirel. Propag. Lett. **19**(1), 84–88 (2020)
5. B.Q. Yang, Z.Q. Yu, Y.Y. Dong, J.Y. Zhou, W. Hong, Compact tapered slot antenna array for 5G millimeter-wave massive MIMO systems. IEEE Antennas Wirel. Propag. Lett. **65**(12), 6721–6727 (2017)
6. D. Chen et al., 2–40 GHz dual-band dual-polarized nested Vivaldi antenna. IEEE Antennas Wirel. Propag. Lett. **13**(2), 163–170 (2019)
7. H.F. Abutarboush, H. Nasif, R. Nilavalan, S.W. Cheung, Multiband and wideband monopole antenna for GSM900 and other wireless applications. IEEE Antennas Wirel. Propag. Lett. **11**, 539–542 (2012)
8. F. Jilani, A.K. Aziz, Q.H. Abbasi, A. Alomainy, *Ka-band flexible Koch fractal antenna with defected ground structure for 5G wearable and conformal applications*, in *IEEE 29th Annual International Symposium Personal, Indoor Mobile Radio Communication* (2018), pp. 361–364
9. S. Kim, R. Yu-Jiun, L. Hoseon, A. Rida, S. Nikolaou, M. Tentzeris, Monopole antenna with inkjet-printed EBG array on paper substrate for wearable applications. IEEE Antennas Wirel. Propag. Lett. **11**, 663–666 (2012)
10. J.K. Ji, G.H. Kim, W.M. Seong, Bandwidth enhancement of metamaterial antennas based on composite right/left-handed transmission line. IEEE Antennas Wirel. Propag. Lett. **9**, 36–39 (2010)
11. X.L. Sun, S.W. Cheung, T.I. Yuk, Dual-band antenna with compact radiator for 2.4/5.2/5.8 GHz WLAN applications. IEEE Antennas Wirel. Propag. Lett. **60**(12), 5924–5931 (2012)
12. H. Wang, L. Liu, Z. Zhang, Y. Li, Z. Feng, A wideband compact WLAN/WiMAX MIMO antenna based on dipole with V-shaped ground branch. IEEE Antennas Wirel. Propag. Lett. **63**(5), 2290–2295 (2015)
13. S. Xiao, M.-C. Tang, Y.-Y. Bai, S. Gao, B.-Z. Wang, Mutual coupling suppression in microstrip array using defected ground structure. IEEE Antennas Wirel. Propag. Lett. **5**(12), 1488–1494 (2011)
14. B. Mukherjee, S.K. Parui, S. Das, *Mutual coupling reduction of microstrip antenna arrays using rectangular split ring-shaped defected ground structure*, in *Proceedings of the International Conference on Communication, Devices Intelligent System* (2012), pp. 202–204
15. A. Habashi, J. Nourinia, C. Ghobadi, Mutual coupling reduction between very closely spaced patch antennas using low-profile folded split-ring resonator. IEEE Antennas Wirel. Propag. Lett. **10**, 862–865 (2011)
16. C.K. Ghosh, B. Mandal, S.K. Parui, Mutual coupling reduction of a dual-frequency microstrip antenna array by using U-shaped DGS and inverted U-shaped microstrip resonator. Prog. Electromagn. Res. C **48**, 61–68 (2014)
17. J. Acharjee, K. Mandal, S.K. Mandal, P.P. Sarkar, *Mutual coupling reduction between microstrip patch antennas by using a string of H-shaped DGS*, in *International Conference on Microelectronics Computing and Communication* (2016), pp. 1–3
18. M.M.B. Suwailam, O.F. Siddiqui, O.M. Ramahi, Mutual coupling reduction between microstrip patch antennas using slotted-complementary split-ring resonators. IEEE Antennas Wirel. Propag. Lett. **9**, 876–878 (2010)
19. P.R. Prajapati, M.V. Kartikeyan, *Proximity coupled stacked circular disc microstrip antenna with reduced size and enhanced*

bandwidth using DGS for WLAN/WiMAX applications, in *IEEE Conference on Electrical, Electronics and Computer Science* (2012), pp. 1–4
20. M.K. Khandelwal, B.K. Kanaujia, S. Kumar, Defected ground structure: Fundamentals, analysis, and applications in modern wireless trends. Int. J. Antennas Propoag **2017**(2017), 2018527 (2017)
21. F. Hattan, W. Abutarboush, A.S. Li, Flexible-screen-printed antenna with enhanced bandwidth by employing defected ground structure. IEEE Antennas Wirel. Propag. Lett. **19**(10), 1803–1807 (2020)
22. K. Sarma, S. Sarmah, K. Goswami, K. Sarma, S. Baruah, *DGS based planer UWB antenna with band rejection features*, in *Proceedings of the International Conference Wireless Communication Signal Processing Networking* (2017), pp. 2640–2644
23. S. Chakraborty, A. Ghosh, S. Chattopadhyay, L.L.K. Singh, Improved cross-polarized radiation and wide impedance bandwidth from rectangular microstrip antenna with dumbbell-shaped defected patch surface. IEEE Antennas Wirel. Propag. Lett. **15**, 84–88 (2016)
24. P. Umar, G. Singh, Gap-coupling: a potential method for enhancing the bandwidth of microstrip antennas. Adv. Comput. Tech. Electromag. **2012**, 1–6 (2012)
25. K. Wei, J.-Y. Li, L. Wang, Z.-J. Xing, R. Xu, Mutual coupling reduction by novel fractal defected ground structure bandgap filter. IEEE Trans. Antennas Propoag. **64**(10), 4328–4335 (2016)
26. K. Gautam, L. Kumar, B.K. Kanaujia, K. Rambabu, Design of compact F-shaped slot triple-band antenna for WLAN/WiMAX applications. IEEE Trans. Antennas Propoag. **64**(3), 1101–1105 (2016)
27. H.-J. Choi, J.-S. Lim, Y.-C. Jeong, A new design of Doherty amplifiers using defected ground structure. IEEE Microw. Wirel. Common. Lett. **16**(12), 87–689 (2006)
28. M.A. Antoniades, G.V. Eleftheriades, A compact multiband monopole antenna with a defected ground plane. IEEE Antennas Wirel. Propag. Lett. **7**, 652–655 (2008)
29. D. Ahn, J.-S. Park, C.-S. Kim, J. Kim, Y. Qian, T. Itoh, A design of the low-pass filter using the novel microstrip defected ground structure. IEEE Trans. Microw. Theory Tech. **49**(1), 86–93 (2001)
30. B.B.Q. Elias, P.J. Soh, A.A. Al-Hadi, P. Akkaraekthalin, G.A.E. Vandenbosch, Bandwidth optimization of a textile PIFA with DGS using characteristic mode analysis. Sensors **21**, 2516 (2021). https://doi.org/10.3390/s21072516
31. Z. Niu, H. Zhang, Q. Chen, T. Zhong, Isolation enhancement for 1–3 closely spaced E-plane patch antenna array using defect ground structure and metal-vias. IEEE Antennas Wirel. Propag. Lett. **7**, 119375–119383 (2019)
32. R.A. Pandhare, P.L. Zade, M.P. Abegaonkar, Miniaturized microstrip antenna array using defected ground structure with enhanced performance. Int. J. Eng. Sci. Technol. **19**(3), 1360–1367 (2016)
33. Di. Gao, Z.-X. Cao, Fu. Sui-Dao, X. Quan, P. Chen, A novel slot-array defected ground structure for decoupling microstrip antenna array. IEEE Trans. Antennas Propag. **68**(10), 7027–7038 (2020)
34. K.N. Olan-Nunez, R.S. Murphy-Arteaga, E. Colin-Beltran, Miniature patch and slot microstrip arrays for IoT and ISM band applications. IEEE Access **08**, 102846–102854 (2020)
35. A.S. Das, A. Goel, S. Nakhate, D. Mitra, Y.K. Gupta, *Wideband patch antenna for stable radiation pattern generation*, in *2023 1st International Conference on Innovations in High Speed Communication and Signal Processing (IHCSP), BHOPAL, India* (2023), pp. 407–410. https://doi.org/10.1109/IHCSP56702.2023.10127133
36. Z. -L. Li, Z. -J. Xing, J. -Y. Li, *A T-shaped defected ground structure for decoupling circularly polarization microstrip antenna array*, in *2021 IEEE International Symposium on Antennas and Propagation and USNC-URSI Radio Science Meeting (APS/URSI), Singapore, Singapore* (2021), pp. 933–934. https://doi.org/10.1109/APS/URSI47566.2021.9703934
37. Y.K. Gupta, A. Geol, Performance analysis of multiple-bean WDM free space laser communication system using homodyne detection approach. Heliyon **9**(2), e13325 (2023)
38. Y.K. Gupta, A. Geol, EDFA controlled spectral efficient MIMO free space optic links for mitigation of climatic turbulence conditions. Wirel. Pers. Commun. **132**, 2563–2585 (2023)
39. Y.K. Gupta, A. Geol, Homodyne detection based multiple-beam WDM FSO communication system under various environmental conditions. Opt. Quantum Electr. **56**(3), 2024 (2024). https://doi.org/10.1007/s11082-023-05835-0
40. W. Chang, S. Chen, K. Chen, P. Yu, Q.H. Liu, Mutual coupling reduction in antenna arrays using the novel mushroom electromagnetic band gap and defected ground structure" Microw. Opt. Technol. Lett. (2024). https://doi.org/10.1002/mop.34084
41. W.J. Lee, W.-S. Yoon, D. Ahn, S.-M. Han, Compact design method for planar antennas with defected ground structures. Electronics **12**, 2226 (2023). https://doi.org/10.3390/electronics12102226
42. E. MousaAli, M. Alibakhshikenari, B.S. Virdee, L. Kouhalvandi, P. Livreri, F. Falcone, An antenna array utilizing slotted conductive slab: inspired by metasurface and defected ground plane techniques for fexible electronics and sensors operating in the millimeter-wave and terahertz spectrum. SN Appl. Sci. **5**, 345 (2023). https://doi.org/10.1007/s42452-023-05570-x